

[SI Appendix]

FBXW7-mediated stability regulation of signal transducer and activator of transcription 2 in melanoma formation

Cheol-Jung Lee¹, Hyun-Jung An¹, Seung-Min Kim¹, Sun-Mi Yoo¹, Juhee Park¹, Ga-Eun Lee¹, Woo-Young Kim², Dae Joon Kim³, Han Chang Kang¹, Joo Young Lee¹, Hye Suk Lee¹, Sung-Jun Cho⁴, and Yong-Yeon Cho^{1,*}

Content

- 1. *SI Appendix*, Supplementary Materials and Methods**
- 2. *SI Appendix*, References**
- 3. *SI Appendix*, 8 Tables**
- 4. *SI Appendix*, 9 Figures**
- 5. *SI Appendix*, Whole blots**

1. SI Appendix, Supplementary Materials and Methods

Cell culture and transfection

293T, HeLa, U2OS, HaCaT, and HCT116 were cultured in Dulbeccos's Modified Eagle's Media (DMEM, ThermoFisher Scientific) supplemented with 10% fetal bovine serum (FBS), 2 mM glutamine (ThermoFisher Scientific), 100 U penicillin, and 100 µg/mL streptomycin (ThermoFisher Scientific). SK-MEL-2, -5, and -28 cells were cultured in Minimal Essential Media (MEM) supplemented with 10% fetal bovine serum (FBS), 2 mM glutamine (ThermoFisher Scientific), 100 U penicillin, and 100 µg/mL streptomycin (ThermoFisher Scientific). The *FBXW7*^{+/+} and *FBXW7*^{-/-} of HCT116 cells were kind gifts from Dr. Bert Vogelstein (Rajagopalan et al., 2004). The cells were maintained at 37°C in a 5% CO₂ incubator. When the cells reached 50% confluence, the plasmids were transfected using jetPEI (Polyplus, New York, NY) following the manufacturer's protocol. At 30 h post-transfection, transfected cells were subjected to Western blotting or immunoprecipitation.

Mammalian two-hybrid assay.

293T cells (2.0 X 10⁴) were seeded into 48-well plates and transfected with pBIND-FBXW7 as the bait, the indicated pACT-transcription factors as the prey, and pG5-luciferase reporter plasmids. Thirty hours after transfection, the cells were disrupted with cell lysis buffer and incubated on an orbital shaker for 30 min. The lysate (20 µl - 40 µl) was transfer to 96-well white luminescence plate, and the luminescence activity was measured automatically with Victor X3 plate reader (PerkinElmer). The relative luciferase activity was calculated and normalized based on the pBIND-FBXW7/pACT-mock/pG5-luciferase basal control. We measured the transfection efficiency and protein concentration via a luciferase assay, Renilla luciferase activity assay, or Lowry protein assay were used.

***In vitro* kinase assay**

In vitro kinase assay was performed as described previously (1). Briefly, the GST fusion STAT2 proteins (2 µg) including GST-STAT4-WT or -4A was combined with commercially active glycogen synthase kinase 3 α (GSK3 α) or GSK3 β purchased from SignalChem in the presence of 100 µM ATP, 10 µCi [γ - 32 P]ATPm, and kinase reaction buffer. The reaction mixture was incubated at 30 °C for 30 min, and the reaction was stopped by adding 6X SDS sample buffer and boiling at 95 °C for 3 min. The 32 P-labeled GST-STAT2 proteins were visualized by autoradiography.

RNA isolation

Total RNA was isolated using Trizol reagent (Invitrogen). The RNA quality was assessed with an Agilent 2100 bioanalyzer using the RNA 6000 Nano Chip (Agilent Technologies, Amstelveen, The Netherlands), and RNA quantification used a ND-2000 Spectrophotometer (Thermo Inc., DE, USA).

GST-STAT2 purification

The pGEX-5x-1-STAT2 plasmid with N-terminal glutathione S-transferase (GST) tag was introduced into Rosetta BL21 competent cells (Merck Millipore Korea, Seoul, Korea). The recombinant GST-STAT2 protein was induced by 0.1 mM of isopropyl β -D-1-thiogalactopyranoside (IPTG) induction for 16 h at 16 °C. The bacterial cell pellets were obtained by centrifugation at 4,000 rpm for 15 min, sonicated in cell lysis buffer, and the supernatant (soluble fraction) was incubated with 50% glutathione-sepharose slurry (GE healthcare Lifescience, Seoul Korea) for 2 h at 4 °C. The beads were washed with PBS buffer and eluted with elution buffer. The eluted GST-STAT2 proteins were used for *in vitro* kinase assays.

Generation of stable cell lines using viral infection

293T cells were used for packaging of lentiviral or retroviral cDNA-expressing viruses to produce viral particles. The viral particles were then used to infect various cell lines. In brief, media containing secreted viruses were collected twice at 24 h and 48 h after transfection, and then filtered with 0.45 µm acetate

syringe filters. Various cell lines were infected with the viruses in the presence of 1 µg/ml polybrene (Sigma Aldrich) and cultured for 48 h. Cells were selected using puromycin (5 µg/ml) or hygromycin B (200 µg/ml) for three days.

Western blot and Immunoprecipitation

Cells were disrupted with lysis buffer (50 mM Tris at pH 8.0, 150 mM NaCl and 0.5% NP-40) and supplemented with protein inhibitor cocktail (Complete Mini, Roche). The cell lysate protein mixtures were measured with spectrophotometer (xMark, BioRad) using the Bio-Rad *DC* Protein Assay kit. Samples containing equal amounts of whole cell lysates were resolved by SDS-PAGE and immunoblotted with indicated antibodies. For immunoprecipitation, 500 µg of lysates were incubated with the 2 µg of indicated antibodies for 4 h or overnight at 4°C followed by 2 h incubation with protein G sepharose beads (GE Healthcare). The immunoprecipitates were washed three times with wash buffer (20 mM Tris at pH 8.0, 100 mM NaCl, 1 mM EDTA, and 0.5% NP-40) resolved by SDS-PAGE and immunoblotted with the indicated antibodies.

Cell proliferation assay

Cell proliferation was measured by MTS (Promega). SK-MEL-2, -5, and 28 cells (2×10^3 /well) were seeded into 96-well plates with 100 µl of culture medium. At each time point, each well was treated with 20 µl of CellTiter 96 Aqueous One Solution. The mixture was incubated for 1 h at 37°C in a 5% CO₂ incubator and then the absorbance at 492 nm was measured using an xMark™ Microplate Absorbance Spectrophotometer (Bio-Rad Laboratories).

Quantitative real-time PCR

HCT116^{FBXW7+/+} and HCT116^{FBXW7-/-} (5×10^5) cells were seeded into a 60-mm dish and cultured overnight. The cells were harvested, and total RNA was extracted by Trizol Reagent (Thermo Fisher Scientific). The

RNA concentration and quality were measured by NanoVue (GE Healthcare Life Sciences), and STAT2 gene expression was analyzed with 50 ng of total RNA using STAT-2 specific real-time primer set (Hs00237139_m1) and glyceraldehyde 3-phosphate dehydrogenase (GAPDH)-specific real-time primer set (Hs02786624_g1). Quantitative real-time PCR was performed by TaqMan RNA-to-Ct™ 1-step kit (Applied Biosystems) following the manufacturer's instructions. The Ct values of STAT2 were normalized with GAPDH as an internal control.

UVB irradiation

Cells were seeded to 80-85% confluence and cultured overnight. The cells were washed with PBS and irradiated with UVB at indicated doses using UV chambers (Opsytec Dr. Grobel GmbH, UV-Elektronik, BS-04). Prewarmed medium was added to cells immediately after UVB irradiation and incubated an additional time before harvest.

Soft agar colony formation assay

Soft agar colony formation was performed with SK-MEL-2, -5, and -28, human melanoma cell lines. Briefly, the cells (8×10^3 /well) were suspended in 1 ml of 0.3% DMEM agar containing 10% FBS. The cultures were maintained at 37 °C in a 5% CO₂ incubator for 2-3 weeks. The colonies were counted using an ECLIPSE Ti inverted microscope and analyzed by NIS-Elements AR (V. 4.0) computer software program (NIKON Instruments Korea, Seoul, Korea).

Skin cancer tissue array (Immunohistofluorescence assay)

Immunohistofluorescence assay was performed as described previously (C.J. Lee, CDD. 2018). A human skin tissue array (SK801) was purchased from US Biomax. Briefly, the slide was deparaffinized by incubation at 60 °C for 2 h, rehydrated, and unmasked by boiling with 10 mM sodium citrate buffer (pH 6.0) for 10 min. After cooling, the slide was blocked with 5% goat serum in 0.5% Triton X-100/PBS for 1 h at

RT and hybridized with the indicated antibodies against STAT2 (100:1) and FBXW7 (100:1) overnight at 4°C. The slide was washed three times and hybridized with secondary antibodies conjugating Alexa-488 and -568 for 2 h at RT. Images were captured using laser scanning confocal microscope (LSM 710), and the intensity was analyzed by Image J computer software program (Ver. 1.6).

STAT2 and FBXW7 docking

Computational STAT2 and FBXW7 docking used a Discovery Studio Ver. 2018 computer program. The crystal structure of FBXW7 (PDB ID: 2VOP) was obtained from human protein database (<https://www.rcsb.org/>). The STAT2 protein structure was built by SWISS-MODEL homology modeling (<https://swissmodel.expasy.org/>) based on the STAT1/DNA complex structure that contained 44.6% amino acid similarity with STAT2 (ID: 1YVL, (2)). The complex structural model of the STAT2-FBXW7 interaction was developed using *in silico* antigen-antibody docking. A rigid-body docking program, ZDOCK (3), with default parameters was used to search all possible binding modes for the antibody and antigen to obtain more accurate predictions for the two proteins by evaluating shape complementarity and desolvation energy. The leading 2,000 predictions from ZDOCK were fed into RDOCK where they were minimized by CHARMM to improve the energy levels and eliminate clashes. The desolvation energy and electrostatics were then recomputed by RDOCK. To further obtain a reliable complex structure in the solvated system, the best prediction from RDOCK was simulated with water molecules and optional counterions to simulate the solvent and minimize and calculate the solvation model in Discovery Studio v 2018. The solvated system can be optionally minimized to eliminate van Der Waals clashes. Finally, the interaction between the WD40 domain of FBXW7 and the degron motifs of the DNA binding domain found in STAT2 was successfully emulated using the complementarity-determining regions (CDRs) of the rational antibody-antigen complex model. The rational antibody-antigen complex model satisfied the complementarity-determining regions (CDRs) of the WD40 domain of FBXW7 interacting with the degron motifs of the STAT2 at the DNA binding domain. STAT2 was compared to STAT1 to identify structural

similarities (1YVL). Acceptable poses of FBXW7 for STAT2 binding at WD40 domains were compared with FBXW7 and cycle E docking (4).

Ampli-Seq Method (Human)

AmpliSeq libraries were constructed and sequenced on the Ion Torrent S5xl platform (Thermo Fisher) according to the manufacturer's instructions. For human gene analysis in cell lines, the Ion AmpliSeq Transcriptome Human Gene Expression Kit is designed for targeted amplification of over 20,000 human RefSeq genes simultaneously in a single primer pool. A short amplicon (~ 110 base pairs (bp)) was amplified for the targeted gene. For each sample, 30 ng of total RNA was used for cDNA library preparation. Multiple libraries were multiplexed and clonally amplified using the Ion Chef System (Thermo Fisher) and then sequenced on an Ion Torrent S5xl machine (Thermo Fisher). The values were normalized using ampliSeq RNA Plug in (ver 5.6.0.3) by Torrent Suite Software (Thermo Fisher).

2. SI Appendix, References

1. Lee CJ, *et al.* (2014) Targeting of magnolin on ERKs inhibits Ras/ERKs/RSK2-signaling-mediated neoplastic cell transformation. *Carcinogenesis* 35(2):432-441.
2. Mao X, *et al.* (2005) Structural bases of unphosphorylated STAT1 association and receptor binding. *Mol Cell* 17(6):761-771.
3. Chen R, Li L, & Weng Z (2003) ZDOCK: an initial-stage protein-docking algorithm. *Proteins* 52(1):80-87.
4. Hao B, Oehlmann S, Sowa ME, Harper JW, & Pavletich NP (2007) Structure of a Fbw7-Skp1-cyclin E complex: multisite-phosphorylated substrate recognition by SCF ubiquitin ligases. *Mol Cell* 26(1):131-143.

3. SI Appendix, Tables

SI Appendix, Table S1. Antibodies use in this research.

antibodies	Source	Identifier
Rabbit polyclonal anti-STAT1	Cell Signaling Technology	Cat# 9172; PRID:AB_2198300
Rabbit monoclonal anti-K48-linkage Ubiquitin	Cell Signaling Technology	Cat# 5621; PRID:AB_10827985
Rabbit monoclonal anti-K63-linkage Ubiquitin	Cell Signaling Technology	Cat# 8081; PRID:AB_10859893
Mouse monoclonal anti-GSK3b	Cell Signaling Technology	Cat# 9832; PRID:AB_10839406
Mouse monoclonal anti-p-SAPK/JNK (T183/Y180)	Cell Signaling Technology	Cat# 9255; PRID:AB_2307321
Mouse monoclonal anti-vp16	Santa Cruz Biotechnology	Cat# sc-7546; PRID:AB_628444
Mouse monoclonal anti-Myc	Santa Cruz Biotechnology	Cat# sc-40; PRID:AB_627268
Rabbit polyclonal anti-Gal4	Santa Cruz Biotechnology	Cat# sc-577; PRID:AB_631554
Mouse monoclonal anti-GST	Santa Cruz Biotechnology	Cat# sc-138; PRID:AB_627677
Mouse monoclonal anti-STAT3	Santa Cruz Biotechnology	Cat# sc-8019; PRID:AB_628293
Mouse monoclonal anti-STAT2	Santa Cruz Biotechnology	Cat# sc-1668; PRID:AB_628291
Mouse monoclonal anti-cyclin E	Santa Cruz Biotechnology	Cat# sc-247; PRID:AB_627357
Mouse monoclonal anti-b-actin	Santa Cruz Biotechnology	Cat# sc-47778; PRID:AB_626632
Mouse monoclonal anti-cullin1	Santa Cruz Biotechnology	Cat# sc-17775; PRID:AB_627325
Mouse monoclonal anti-c-Myc	Santa Cruz Biotechnology	Cat# sc-373712; PRID:AB_10916994
Mouse monoclonal anti-Flag	Sigma-Aldrich	Cat# F1804; RRID: AB_262044
Mouse monoclonal anti-HA agarose beads	Sigma-Aldrich	Cat# A-2095; RRID: AB_257974
Mouse monoclonal anti-HisG-HRP	Thermo Fisher Scientific	Cat# R941-25 RRID: AB_2556558
Mouse monoclonal anti-Xpress	Thermo Fisher Scientific	Cat# R910-25 RRID: AB_2556552
Rabbit polyclonal anti-FBXW7	Bethyl Laboratories	Cat# A301-720A; RRID: AB_1210897
Mouse monoclonal anti-HA-HRP	MBL International	Cat# M180-7; RRID: AB_11124961

SI Appendix, Table S2. Chemicals and proteins utilized in this research.

Chemicals, Recombinant proteins	Source	Identifier
MLN4924	Calbiochem	Cat# 505477
MG132	Sigma-Aldrich	Cat# C2211
cycloheximide	Sigma-Aldrich	Cat# 01810
Alkaline phosphatase	New England BioLabs	Cat# M0290S
CHIR99021 (GSK3 inhibitor)	Selleckchem	Cat# S1263
GSK3a, Active	Signalchem	Cat# G08-10G
GSK3b, Active	Signalchem	Cat# G09-10G

SI Appendix, Table S3. Assay kits utilized in this research.

Critical commercial Assays	Source	Identifier
Site-specific Mutagenesis Kit	ELPIS-BIOTECH	Cat# EBT-5001
Quick Start Bradford 1x Dye Reagent	BIO-RAD	Cat# 500-0205

SI Appendix, Table S4. List for Information of bacterial strains utilized in this article.

Bacterial Strains	Source	Identifier
DH5a	enzynomics	
BL21	enzynomics	

SI Appendix, Table S5. Mammalian cell lines used in this research.

Experimental Models: Cell Lines	Source	Identifier
293T	ATCC	
Hela	ATCC	
U2OS	ATCC	
HCT116 FBXW7 ^{+/+} and FBXW7 ^{-/-}	Rajagopalan et al., 2004	
WM2664	Korean Cell Line Bank	
A375-SM	Korean Cell Line Bank	
HS294T	Korean Cell Line Bank	

SK-MEL-2	ATCC	
SK-MEL-5	ATCC	
SK-MEL-28	ATCC	
HaCaT	ATCC	

SI Appendix, Table S6. Plasmids utilized in this research.

Recombinant DNA	Source	Identifier
shRNA FBW7-1	Dharmacon	TRCN0000006556
shRNA FBW7-2	Dharmacon	TRCN0000006558
shRNA Cullin1-1	Dharmacon	TRCN0000003391
shRNA Cullin1-2	Dharmacon	TRCN0000003392
shRNA STAT2	Dharmacon	TRCN0000007460
plasmid Myc-Cullin1	Addgene	#19896
plasmid Myc-Cullin2	Addgene	#19892
plasmid Myc-Cullin3	Addgene	#19893
plasmid Myc-Cullin4A	Addgene	#19951
plasmid Myc-Cullin4B	Addgene	#19922
plasmid Myc-Cullin7	Addgene	#20695
plasmid Myc-RBX1	Addgene	#20717
plasmid Flag-bTrcp1	Dr. Michele Pagano	
plasmid Flag-FBXW2	Dr. Michele Pagano	
plasmid Flag-FBXW7	Dr. Michele Pagano	
plasmid Gal4-FBXL1	Korea Human Gene Bank	hMU008256
plasmid Gal4-FBXL8	Korea Human Gene Bank	hMU011707
plasmid Gal4-FBXL9	Korea Human Gene Bank	hMU013084
plasmid Gal4-FBXO4	Korea Human Gene Bank	KU026612
plasmid Gal4-FBXO6	Korea Human Gene Bank	hMU013630
plasmid Gal4-FBXO17	Korea Human Gene Bank	hMU001519
plasmid Xp/His-STAT2	This paper	N/A
plasmid Xp/His-STAT2 1-698	This paper	N/A
plasmid Xp/His-STAT2 1-574	This paper	N/A
plasmid Xp/His-STAT2 1-315	This paper	N/A
plasmid Xp/His-STAT2 1-139	This paper	N/A

plasmid Xp/His-STAT2 Δ140	This paper	N/A
plasmid Xp/His-STAT2 Δ316	This paper	N/A
plasmid Xp/His-STAT2 Δ575	This paper	N/A
plasmid Xp/His-STAT2 Δ699	This paper	N/A
plasmid Xp/His-STAT2 N	This paper	N/A
plasmid Xp/His-STAT2 C-C	This paper	N/A
plasmid Xp/His-STAT2 DNA	This paper	N/A
plasmid Xp/His-STAT2 SH2	This paper	N/A
plasmid Xp/His-STAT2 T	This paper	N/A
plasmid Xp/His-STAT2 ΔC-C	This paper	N/A
plasmid Xp/His-STAT2 ΔDNA	This paper	N/A
plasmid Xp/His-STAT2 ΔC-C/DNA	This paper	N/A
plasmid Xp/His-STAT2 3A (S381A/T385A/E389A)	This paper	N/A
plasmid Xp/His-STAT2 4A (S381A/T385A/E389A/S393A)	This paper	N/A
plasmid myc-FBXW7 N278	This paper	N/A
plasmid myc-FBXW7 N324	This paper	N/A
plasmid myc-FBXW7 C325	This paper	N/A
HA-GSK3b	Addgene	#14753
HA-CK1	Korea Human Gene Bank	N/A
His-ERK	Korea Human Gene Bank	N/A
Gal4-p38	Korea Human Gene Bank	N/A

SI Appendix, Table S7. Details on the tissue array samples.

position	sex	age	organ	pathology	grade	image	type	FBXW7(red intensity)	STAT2 (Green intensity)
A1	M	45	Skin	Squamous carcinoma cell	II	http://www.biomax.us/tissue-array-image.php?catalognum=SK801&number=1	Malignant	12.0	43.0
A2	M	47	Skin	Squamous carcinoma cell	II	http://www.biomax.us/tissue-array-image.php?catalognum=SK801&number=2	Malignant	11.5	24.6
A3	M	66	Skin	Squamous carcinoma cell	I	http://www.biomax.us/tissue-array-image.php?catalognum=SK801&number=3	Malignant	6.1	34.3
A4	M	71	Skin	Chronic inflammation of fibrous tissue	-	http://www.biomax.us/tissue-array-image.php?catalognum=SK801&number=4	Malignant	8.2	24.8
A5	M	52	Skin	Malignant melanoma	-	http://www.biomax.us/tissue-array-image.php?catalognum=SK801&number=5	Malignant	11.5	18.3
A6	F	75	Skin	Malignant melanoma	-	http://www.biomax.us/tissue-array-image.php?catalognum=SK801&number=6	Malignant	14.2	53.3
A7	M	53	Skin	Malignant melanoma	-	http://www.biomax.us/tissue-array-image.php?catalognum=SK801&number=7	Malignant	9.9	25.9
A8	M	70	Skin	Squamous carcinoma cell	I	http://www.biomax.us/tissue-array-image.php?catalognum=SK801&number=8	Malignant	8.4	19.4
A9	F	80	Skin	Squamous carcinoma cell	I	http://www.biomax.us/tissue-array-image.php?catalognum=SK801&number=9	Malignant	10.2	38.4
A10	M	37	Skin	Squamous carcinoma cell	I	http://www.biomax.us/tissue-array-image.php?catalognum=SK801&number=10	Malignant	9.3	40.7

				carcinoma			image.php?catalognum=SK801&number=10			
B1	F	85	Skin	Squamous carcinoma	cell	I	http://www.biomedpub.com/submit/submitImage.php?catalognum=SK801&number=11	Malignant	6.7	67.8
B2	M	65	Skin	Squamous carcinoma	cell	I	http://www.biomedpub.com/submit/submitImage.php?catalognum=SK801&number=12	Malignant	6.6	72.3
B3	M	62	Skin	Squamous carcinoma	cell	I	http://www.biomedpub.com/submit/submitImage.php?catalognum=SK801&number=13	Malignant	5.7	70.3
B4	M	61	Skin	Squamous carcinoma	cell	I	http://www.biomedpub.com/submit/submitImage.php?catalognum=SK801&number=14	Malignant	7.6	41.4
B5	F	86	Skin	Chronic inflammation of skin tissue		-	http://www.biomedpub.com/submit/submitImage.php?catalognum=SK801&number=15	Malignant	8.5	35.4
B6	M	34	Skin	Squamous carcinoma	cell	I	http://www.biomedpub.com/submit/submitImage.php?catalognum=SK801&number=16	Malignant	9.2	62.7
B7	F	56	Skin	Squamous carcinoma	cell	I	http://www.biomedpub.com/submit/submitImage.php?catalognum=SK801&number=17	Malignant	6.4	47.6
B8	F	79	Skin	Squamous carcinoma	cell	I	http://www.biomedpub.com/submit/submitImage.php?catalognum=SK801&number=18	Malignant	9.2	33.3
B9	F	55	Skin	Squamous carcinoma	cell	I	http://www.biomedpub.com/submit/submitImage.php?catalognum=SK801&number=19	Malignant	10.4	46.4
B10	M	73	Skin	Squamous carcinoma	cell	I	http://www.biomedpub.com/submit/submitImage.php?catalognum=SK801&number=20	Malignant	8.3	18.3
C1	M	61	Skin	Squamous carcinoma	cell	I	http://www.biomedpub.com/submit/submitImage.php?catalognum=SK801&number=21	Malignant	13.0	68.2
C2	M	72	Skin	Squamous carcinoma	cell	II	http://www.biomedpub.com/submit/submitImage.php?catalognum=SK801&number=22	Malignant	9.8	53.0
C3	M	74	Skin	Squamous carcinoma	cell	II	http://www.biomedpub.com/submit/submitImage.php?catalognum=SK801&number=23	Malignant	4.4	21.6
C4	M	59	Skin	Squamous carcinoma	cell	II	http://www.biomedpub.com/submit/submitImage.php?catalognum=SK801&number=24	Malignant	X	X
C5	M	65	Skin	Squamous carcinoma	cell	II	http://www.biomedpub.com/submit/submitImage.php?catalognum=SK801&number=25	Malignant	11.5	60.7
C6	M	31	Skin	Squamous carcinoma	cell	I	http://www.biomedpub.com/submit/submitImage.php?catalognum=SK801&number=26	Malignant	6.7	15.6
C7	M	76	Skin	Squamous carcinoma	cell	I	http://www.biomedpub.com/submit/submitImage.php?catalognum=SK801&number=27	Malignant	7.7	38.5
C8	F	84	Skin	Squamous carcinoma	cell	II	http://www.biomedpub.com/submit/submitImage.php?catalognum=SK801&number=28	Malignant	7.5	32.9
C9	M	46	Skin	Squamous carcinoma	cell	III	http://www.biomedpub.com/submit/submitImage.php?catalognum=SK801&number=29	Malignant	X	X
C10	F	62	Skin	Squamous carcinoma	cell	II	http://www.biomedpub.com/submit/submitImage.php?catalognum=SK801&number=30	Malignant	15.8	37.1
D1	M	73	Skin	Squamous carcinoma	cell	II	http://www.biomedpub.com/submit/submitImage.php?catalognum=SK801&number=31	Malignant	8.4	19.2
D2	F	64	Skin	Squamous carcinoma	cell	II	http://www.biomedpub.com/submit/submitImage.php?catalognum=SK801&number=32	Malignant	7.5	34.6
D3	F	90	Skin	Squamous carcinoma	cell	II	http://www.biomedpub.com/submit/submitImage.php?catalognum=SK801&number=33	Malignant	6.6	29.8
D4	M	68	Skin	Squamous carcinoma	cell	II	http://www.biomedpub.com/submit/submitImage.php?catalognum=SK801&number=34	Malignant	6.6	10.2
D5	M	78	Skin	Squamous carcinoma	cell	II	http://www.biomedpub.com/submit/submitImage.php?catalognum=SK801&number=35	Malignant	10.9	35.9
D6	M	51	Skin	Squamous carcinoma	cell	II	http://www.biomedpub.com/submit/submitImage.php?catalognum=SK801&number=36	Malignant	8.8	51.0
D7	M	58	Skin	Squamous carcinoma	cell	II	http://www.biomedpub.com/submit/submitImage.php?catalognum=SK801&number=37	Malignant	6.0	45.2
D8	M	58	Skin	Squamous carcinoma	cell	II	http://www.biomedpub.com/submit/submitImage.php?catalognum=SK801&number=38	Malignant	7.7	51.5
D9	M	67	Skin	Squamous carcinoma	cell	II	http://www.biomedpub.com/submit/submitImage.php?catalognum=SK801&number=39	Malignant	X	X
D10	M	67	Skin	Squamous carcinoma	cell	II	http://www.biomedpub.com/submit/submitImage.php?catalognum=SK801&number=40	Malignant	7.4	12.4
E1	M	54	Skin	Squamous carcinoma	cell	I	http://www.biomedpub.com/submit/submitImage.php?catalognum=SK801&number=41	Malignant	9.9	22.6
E2	M	67	Skin	Squamous carcinoma	cell	II	http://www.biomedpub.com/submit/submitImage.php?catalognum=SK801&number=42	Malignant	7.0	53.4
E3	F	66	Skin	Squamous carcinoma	cell	III	http://www.biomedpub.com/submit/submitImage.php?catalognum=SK801&number=43	Malignant	6.3	14.4
E4	M	45	Skin	Squamous carcinoma	cell	III	http://www.biomedpub.com/submit/submitImage.php?catalognum=SK801&number=44	Malignant	5.6	19.2
E5	M	72	Skin	Squamous carcinoma	cell	III	http://www.biomedpub.com/submit/submitImage.php?catalognum=SK801&number=45	Malignant	11.3	45.6
E6	M	70	Skin	Basal carcinoma	cell	-	http://www.biomedpub.com/submit/submitImage.php?catalognum=SK801&number=46	Malignant	11.3	54.1
E7	M	48	Skin	Basal carcinoma	cell	-	http://www.biomedpub.com/submit/submitImage.php?catalognum=SK801&number=47	Malignant	8.5	18.1
E8	F	74	Skin	Basal carcinoma	cell	-	http://www.biomedpub.com/submit/submitImage.php?catalognum=SK801&number=48	Malignant	7.9	14.1
E9	M	40	Skin	Basal carcinoma	cell	-	http://www.biomedpub.com/submit/submitImage.php?catalognum=SK801&number=49	Malignant	7.7	9.8
E10	M	75	Skin	Basal carcinoma	cell	-	http://www.biomedpub.com/submit/submitImage.php?catalognum=SK801&number=50	Malignant	X	X
F1	M	48	Skin	Basal carcinoma	cell	-	http://www.biomedpub.com/submit/submitImage.php?catalognum=SK801&number=51	Malignant	9.0	26.7
F2	M	60	Skin	Basal carcinoma	cell	-	http://www.biomedpub.com/submit/submitImage.php?catalognum=SK801&number=52	Malignant	14.9	47.4
F3	M	71	Skin	Basal carcinoma	cell	-	http://www.biomedpub.com/submit/submitImage.php?catalognum=SK801&number=53	Malignant	6.4	24.2
F4	M	63	Skin	Basal carcinoma	cell	-	http://www.biomedpub.com/submit/submitImage.php?catalognum=SK801&number=54	Malignant	10.7	23.8

F5	F	73	Skin	Basal carcinoma cell	-	http://www.biomax.us/tissue-array-image.php?catalognum=SK801&number=55	Malignant	10.7	11.7
F6	M	67	Skin	Basal carcinoma cell	-	http://www.biomax.us/tissue-array-image.php?catalognum=SK801&number=56	Malignant	11.3	24.8
F7	F	57	Skin	Basal carcinoma cell	-	http://www.biomax.us/tissue-array-image.php?catalognum=SK801&number=57	Malignant	10.0	15.7
F8	M	76	Skin	Basal carcinoma cell	-	http://www.biomax.us/tissue-array-image.php?catalognum=SK801&number=58	Malignant	12.1	21.0
F9	F	82	Skin	Basal carcinoma cell	-	http://www.biomax.us/tissue-array-image.php?catalognum=SK801&number=59	Malignant	10.1	9.9
F10	F	47	Skin	Malignant melanoma	-	http://www.biomax.us/tissue-array-image.php?catalognum=SK801&number=60	Malignant	11.3	36.7
G1	M	62	Skin	Malignant melanoma	-	http://www.biomax.us/tissue-array-image.php?catalognum=SK801&number=61	Malignant	10.5	22.0
G2	F	43	Skin	Malignant melanoma	-	http://www.biomax.us/tissue-array-image.php?catalognum=SK801&number=62	Malignant	19.0	47.0
G3	M	45	Skin	Malignant melanoma	-	http://www.biomax.us/tissue-array-image.php?catalognum=SK801&number=63	Malignant	12.3	26.4
G4	M	25	Skin	Malignant melanoma	-	http://www.biomax.us/tissue-array-image.php?catalognum=SK801&number=64	Malignant	11.4	20.0
G5	M	49	Skin	Malignant melanoma	-	http://www.biomax.us/tissue-array-image.php?catalognum=SK801&number=65	Malignant	11.0	24.5
G6	F	66	Skin	Malignant melanoma	-	http://www.biomax.us/tissue-array-image.php?catalognum=SK801&number=66	Malignant	7.9	21.0
G7	M	71	Skin	Malignant melanoma	-	http://www.biomax.us/tissue-array-image.php?catalognum=SK801&number=67	Malignant	7.9	21.0
G8	F	72	Skin	Malignant melanoma	-	http://www.biomax.us/tissue-array-image.php?catalognum=SK801&number=68	Malignant	9.7	13.5
G9	M	64	Skin	Sweat gland carcinoma	-	http://www.biomax.us/tissue-array-image.php?catalognum=SK801&number=69	Malignant	5.6	11.1
G10	F	65	Skin	Malignant trichoepithelioma	-	http://www.biomax.us/tissue-array-image.php?catalognum=SK801&number=70	Malignant	9.6	20.8
H1	M	45	Skin	Matched normal skin tissue of No. 01	-	http://www.biomax.us/tissue-array-image.php?catalognum=SK801&number=71	Normal	30.5	10.1
H2	M	47	Skin	Matched normal skin tissue of No. 02	-	http://www.biomax.us/tissue-array-image.php?catalognum=SK801&number=72	Normal	15.1	7.8
H3	M	66	Skin	Matched normal skin tissue of No. 03	-	http://www.biomax.us/tissue-array-image.php?catalognum=SK801&number=73	Normal	18.5	15.7
H4	M	71	Skin	Matched normal skin tissue of No. 04	-	http://www.biomax.us/tissue-array-image.php?catalognum=SK801&number=74	Normal	18.3	0.0
H5	M	52	Skin	Matched normal skin tissue of No. 05	-	http://www.biomax.us/tissue-array-image.php?catalognum=SK801&number=75	Normal	33.7	18.2
H6	F	75	Skin	Matched normal skin tissue of No. 06	-	http://www.biomax.us/tissue-array-image.php?catalognum=SK801&number=76	Normal	20.4	10.1
H7	M	53	Skin	Matched normal skin tissue of No. 07	-	http://www.biomax.us/tissue-array-image.php?catalognum=SK801&number=77	Normal	35.4	25.2
H8	M	63	Skin	Unmatched normal skin tissue	-	http://www.biomax.us/tissue-array-image.php?catalognum=SK801&number=78	Normal	22.7	8.2
H9	M	73	Skin	Unmatched Keratotic matter	-	http://www.biomax.us/tissue-array-image.php?catalognum=SK801&number=79	Normal	12.1	20.3
H10	M	42	Skin	Unmatched normal skin tissue	-	http://www.biomax.us/tissue-array-image.php?catalognum=SK801&number=80	Normal	28.6	0.5

SI Appendix, Table S8. List of putative STAT2 target genes from RNA-Seq analysis.

	genes	F7-wt	F7-KO	F7-KO (shS-S2)
1	ABCB8	0.83268	0.5736	-1.406280851
2	ACAA1	1.001115	-1.36562	0.364500824
3	ADAMTS3	NaN	NaN	NaN
4	ADAMTS6	-0.62666	1.411271	-0.784607462
5	ADPRHL2	1.391834	-0.91294	-0.478893574
6	AIM2	-0.70711	-0.70711	1.414213562
7	AKT2	-1.38237	0.949627	0.432742085
8	ANKFY1	1.275362	-1.16691	-0.108447229
9	ANKRD45	-1.40566	0.568355	0.83730825
10	ANXA2R	0.009314	-1.22938	1.220061251
11	APOL1	-1.38759	0.930315	0.457277483
12	APOL2	-0.598	1.408864	-0.810862048
13	APOL6	1.378654	-0.96225	-0.416407969
14	ARHGAP11B	-1.33746	0.270747	1.066717
15	ARL5B	-1.22451	1.224977	-0.000464078

16	ARRDC4	1.275519	-1.16671	-0.108809768
17	ATP13A1	-0.88963	-0.50725	1.396875756
18	AZI2	1.209726	-1.23923	0.029505397
19	B2M	1.148618	-1.28881	0.140188657
20	BAG1	1.328835	-1.08352	-0.245313955
21	BAK1	0.879279	-1.39888	0.519605802
22	BATF2	1.412742	-0.6505	-0.762236882
23	BLZF1	-1.39892	0.519813	0.879104616
24	BRCA2	-1.28868	0.139881	1.148798642
25	BST2	1.39672	-0.50632	-0.890401577
26	BUB1	-0.78554	-0.62566	1.411197655
27	C14orf159	-0.13565	-1.15127	1.286922349
28	C17orf62	1.235325	-1.21388	-0.021442409
29	C19orf66	1.366408	-0.99895	-0.36745666
30	C5orf48	NaN	NaN	NaN
31	CBX3	-0.7071	-0.70711	1.414213562
32	CCDC9	-1.3801	0.957437	0.422661763
33	CD274	-1.35419	0.324061	1.030126422
34	CD33	1.402631	-0.54489	-0.857744513
35	CD68	-0.65351	-0.75938	1.412892156
36	CDK17	-1.2614	0.07694	1.184461247
37	CHMP5	-1.3801	0.422679	0.957423121
38	CMPK2	1.281768	-1.15838	-0.123387577
39	CNP	1.402968	-0.54734	-0.855626517
40	CREBRF	-0.63684	1.411959	-0.775114172
41	CRKL	1.384342	-0.44178	-0.942566707
42	CSFI	-1.32174	1.096477	0.225262623
43	CUTA	0.08361	1.180797	-1.264407767
44	CWF19L1	-1.03226	-0.32102	1.35328364
45	DCLRE1C	0.422876	0.957271	-1.380147601
46	DCP1A	-0.84128	1.405112	-0.563832254
47	DDX3X	1.36222	-1.01015	-0.352069427
48	DDX58	-1.38072	0.425403	0.955319764
49	DDX60	-1.38305	0.43581	0.9472356
50	DDX60L	-1.3909	0.916917	0.473983137
51	DGCR8	0.76856	0.643819	-1.412378575
52	DGKE	-1.11517	1.310777	-0.195607329
53	DHX15	-1.35594	0.330004	1.025931345
54	DHX58	0.331662	-1.35642	1.024757071
55	DNAJA1	1.402264	-0.86001	-0.542257205
56	DTX3L	0.903343	-1.394	0.490654215
57	EARS2	1.363966	-1.00555	-0.358411191
58	ECE1	-1.37565	0.9719	0.403744772
59	EHD4	-1.41341	0.748091	0.665315007
60	EIF2AK2	1.314216	-0.20475	-1.109464723
61	ENY2	1.413844	-0.67891	-0.734935868
62	EPSTI1	-1.08877	-0.23724	1.326009071
63	EXOSC9	-1.36203	1.010655	0.351370736
64	FAM20B	-0.27336	1.338327	-1.064966855
65	FAM46A	1.289499	-1.14764	-0.141863084
66	FBXO36	-1.39871	0.880201	0.518509911
67	FOXP1	-1.33528	1.071091	0.264187197
68	GCLM	0.069322	-1.25793	1.188611538
69	GMPR	0.614519	0.795816	-1.410334668
70	GNB4	-1.39451	0.900968	0.493546176
71	GNG5	1.351192	-0.31406	-1.037134829
72	GSTK1	-1.41322	0.75247	0.660751994
73	GTPBP2	-1.38592	0.936712	0.44921034
74	HELZ2	-1.4136	0.670757	0.742844237
75	HEMGN	NaN	NaN	NaN
76	HERC5	-1.38099	0.954402	0.42658951
77	HERC6	-1.33209	1.077331	0.254755749
78	HEXDC	-1.41183	0.776957	0.6348756
79	HIRA	0.48815	-1.39355	0.905395468
80	HLA-E	1.414049	-0.72568	-0.688365813
81	HNRNPA2B1	-1.11066	1.313501	-0.202837776

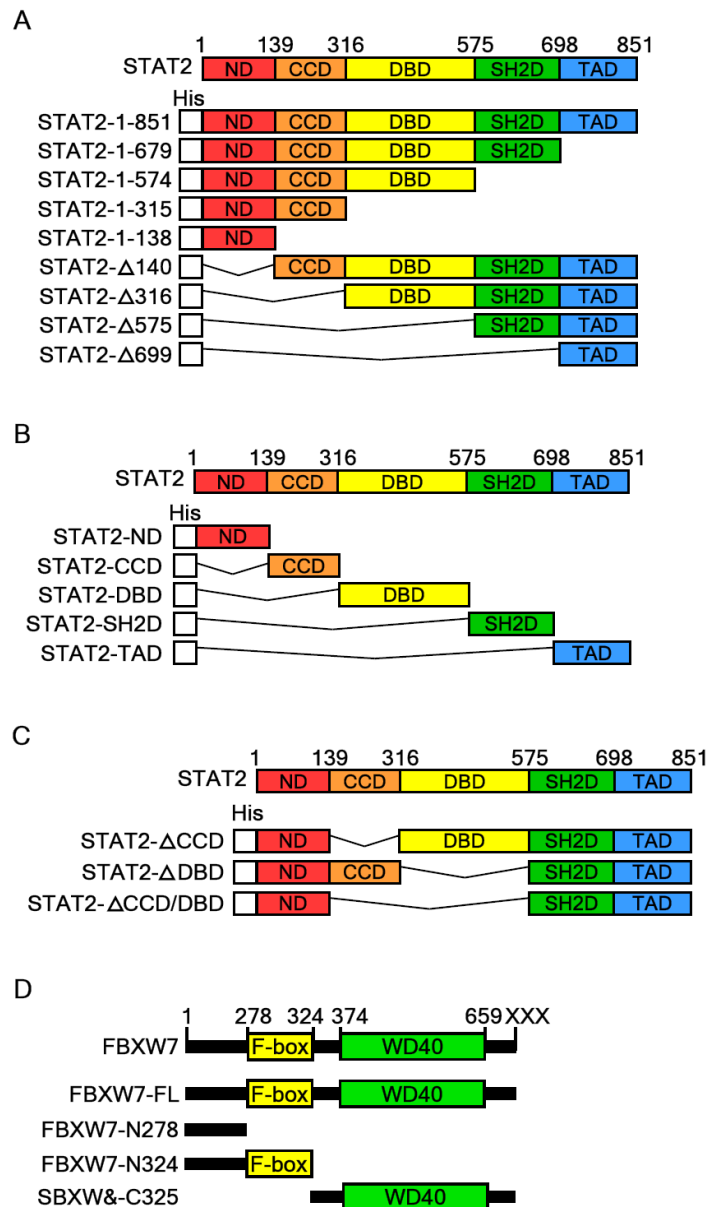
82	HNRNPD	-0.95367	-0.42753	1.381204371
83	HNRNPR	-1.31998	1.099575	0.220407718
84	HSPA1L	-0.70711	1.414214	-0.707106781
85	ICAM1	0.639002	-1.41209	0.773091286
86	IFI16	1.368948	-0.99186	-0.377087557
87	IFI27	1.411803	-0.77739	-0.63441571
88	IFI35	-1.0383	-0.31239	1.350685332
89	IFI44L	1.414214	-0.70711	-0.707106781
90	IFI6	1.412563	-0.64712	-0.76544241
91	IFIH1	-0.57471	-0.8317	1.406409105
92	IFIT1	0.848584	-1.40405	0.555467754
93	IFIT2	1.312411	-1.11248	-0.199935884
94	IFIT3	0.297769	-1.34617	1.048404109
95	IFIT5	1.236348	-1.2128	-0.023545012
96	IFITM1	1.405163	-0.56424	-0.840923679
97	IFITM2	1.367919	-0.37316	-0.994763296
98	IFITM3	1.413735	-0.67501	-0.738723374
99	IRF1	-1.41416	0.695972	0.718183641
100	IRF2	1.296257	-1.13781	-0.158447434
101	IRF7	-0.80566	-0.60374	1.409399941
102	IRF9	1.404847	-0.5617	-0.843148061
103	ISG15	-1.38545	0.938495	0.44695116
104	ISG20	-1.25307	1.194305	0.058763899
105	KCTD14	1.389844	-0.46854	-0.921305595
106	KIF2A	0.848681	0.555356	-1.404037042
107	KLHL6	NaN	NaN	NaN
108	LAP3	1.28039	-0.12015	-1.160244441
109	LGALS3BP	1.092392	-1.32402	0.231628371
110	LGALS9	1.32296	-1.0943	-0.228661459
111	LNPEP	0.5636	0.841484	-1.405083726
112	LOC648691	-1.37539	0.402683	0.972704623
113	LOC728743	1.300846	-0.16995	-1.130891759
114	MAD2L1BP	-0.0372	-1.20572	1.242919402
115	MAGOHB	-1.37915	0.418536	0.960612792
116	MAK	-1.06413	1.338738	-0.274609065
117	MDC1	0.144569	-1.29061	1.146044247
118	MED16	1.021895	0.335692	-1.357586878
119	MOV10	1.163323	0.114765	-1.278088042
120	MRPL40	-1.26181	0.077848	1.18396377
121	MT2A	0.897084	0.498258	-1.395341974
122	MUC1	-1.35987	0.34367	1.01619657
123	MX1	1.355898	-0.32987	-1.026024118
124	MX2	-0.70711	1.414214	-0.707106781
125	MYD88	1.348955	-1.04223	-0.306728381
126	N4BP1	-1.24895	0.049938	1.199012054
127	NADK	-1.37671	0.968525	0.408188657
128	NAMPT	1.289654	-1.14741	-0.14223948
129	NAPA	1.18392	-1.26185	0.077927414
130	NBN	-0.91759	-0.47315	1.390740195
131	NCOA7	1.119898	0.187963	-1.307860394
132	NKAIN1	1.411852	-0.63518	-0.776669646
133	NME7	-1.20504	-0.0385	1.243540108
134	NUDCD1	0.6325	-1.41168	0.779176053
135	OAS1	1.408617	-0.59546	-0.813160744
136	OAS2	NaN	NaN	NaN
137	OAS3	1.397696	-0.51221	-0.885488109
138	OASL	-1.21133	-0.0264	1.237729313
139	OGFOD3	1.315727	-0.20881	-1.106914236
140	OGFR	1.338316	-1.06499	-0.273327753
141	PARP10	1.411763	-0.77795	-0.633811585
142	PARP12	1.331275	-1.07889	-0.252383281
143	PARP14	1.413562	-0.66961	-0.743949641
144	PARP9	1.413071	-0.65732	-0.7557467
145	PGAM1	1.40894	-0.5988	-0.81014341
146	PHF11	1.288457	-1.14911	-0.139343757
147	PI4K2B	-0.89038	-0.50635	1.396724837

148	PML	1.338586	-1.06444	-0.274146552
149	PNPT1	1.403557	-0.55171	-0.851846932
150	PNRC2	-1.35026	0.310987	1.039271992
151	POLR1B	-0.58105	-0.82607	1.407120987
152	POU3F2	-0.82155	-0.58612	1.407666424
153	PPP2R2A	-1.35225	0.317553	1.034693499
154	PRAME	0.091571	1.176389	-1.267960384
155	PRKCE	-1.39612	0.893332	0.502791491
156	PSMA3	0.011697	-1.23055	1.218854431
157	RANBP1	-1.03572	-0.31608	1.351804417
158	RBBP6	-1.23348	0.017655	1.215821692
159	RBCK1	-0.61073	1.410017	-0.799288869
160	RBM43	0.757006	-1.41301	0.656004905
161	RFC2	1.307107	-0.186	-1.121104506
162	RSAD2	1.21208	-1.23703	0.024949273
163	RTP4	-0.70711	-0.70711	1.414213562
164	SAMD9	-0.0761	-1.18492	1.26102026
165	SAMD9L	1.414214	-0.70711	-0.707106781
166	SAMHD1	1.414138	-0.71971	-0.694427158
167	SAPI30	-1.4007	0.869248	0.531453498
168	SCAMP1	0.769323	-1.41233	0.643008567
169	SCN9A	-1.34577	1.04928	0.296492074
170	SCYL3	1.244829	-0.04121	-1.203620933
171	SDE2	-1.40948	0.804881	0.604597537
172	SEMA4B	0.610533	-1.41	0.799467342
173	SLC25A44	-1.27674	0.111637	1.165104273
174	SLFN12	-0.98047	1.372851	-0.392386016
175	SLFN5	-1.06756	-0.26949	1.337047927
176	SMARCA5	-1.07535	-0.25776	1.333110888
177	SNORA67	1.296197	-0.1583	-1.137899553
178	SP100	-1.19208	-0.06291	1.254986539
179	SP110	-1.01429	-0.34632	1.360614275
180	SP140L	-1.03796	-0.31287	1.350832316
181	SSBP1	-0.78903	-0.62189	1.410917587
182	SSR1	-1.36359	1.006557	0.35703138
183	STARD5	0.362052	1.002903	-1.36495542
184	STAT1	-0.82432	1.407334	-0.583012186
185	STAT2	-1.18653	1.259683	-0.073154657
186	STAT3	-1.07775	-0.25412	1.331870816
187	STX16	-1.36786	0.994925	0.372935414
188	SYNGAP1	1.034946	0.317191	-1.352137548
189	TDRD7	-1.24901	1.19895	0.050055378
190	TMEM140	0.568355	-1.40566	0.83730825
191	TMEM62	-1.01954	-0.33899	1.358534812
192	TMPO	-1.21841	-0.01258	1.230987293
193	TNFSF10	-1.25776	1.188816	0.068945091
194	TOR1AIP1	0.85456	-1.40314	0.548575823
195	TRIM14	1.39697	-0.88916	-0.507811261
196	TRIM21	1.029129	-1.35461	0.325477601
197	TRIM22	-1.40715	0.581313	0.825836095
198	TRIM25	-0.34583	-1.01465	1.360475023
199	TRIM38	0.451698	0.934744	-1.38644222
200	TRIM5	-0.76767	1.412432	-0.644759708
201	TRIM56	1.195035	0.057401	-1.252435967
202	TRIP12	0.067107	-1.25692	1.189811936
203	TRMT2A	1.305758	-1.12325	-0.182508893
204	TXNIP	NaN	NaN	NaN
205	UBA7	-0.46261	1.38867	-0.926061651
206	UBE2L6	1.352014	-0.31678	-1.035233183
207	UBFD1	1.411039	-0.78754	-0.623496598
208	UBR1	1.323583	-0.2304	-1.093180607
209	UNC93B1	-1.41142	0.782645	0.628775627
210	UNK	-1.09702	1.321432	-0.224408636
211	USF1	1.273527	-1.1693	-0.104226055
212	USP18	1.313895	-1.11	-0.203890484
213	WARS	-0.96405	-0.41406	1.378104326

214	WBP4	-1.07824	-0.25338	1.331615738
215	WDR25	-0.89636	1.395493	-0.499128827
216	XAF1	-0.70711	1.414214	-0.707106781
217	XRN1	-1.10573	-0.2107	1.316425848
218	YDJC	1.149509	-1.28818	0.138667291
219	ZC3HAV1	1.360968	-0.34758	-1.013387426
220	ZNF107	1.175445	-1.26871	0.093266352
221	ZNFX1	1.013532	-1.36091	0.347378938

4. SI Appendix, Figures

SI Appendix, Figure S1



SI Appendix, Figure S1. Construction strategies of deletion expression vectors for STAT2 and FBXW7.

(A) Construction strategies for serial deletion mutants of STAT2. (B) Construction strategies for each domain of STAT2. (C) Construction strategies for domain-specific deletion mutants of STAT2. (D) Construction strategies for deletion mutants of FBXW7. (A-C) ND, N-terminal domain; CCD, coiled-coil domain; DBD, DNA binding domain; SH2D, SH2 domain; and TAD, transactivation domain.

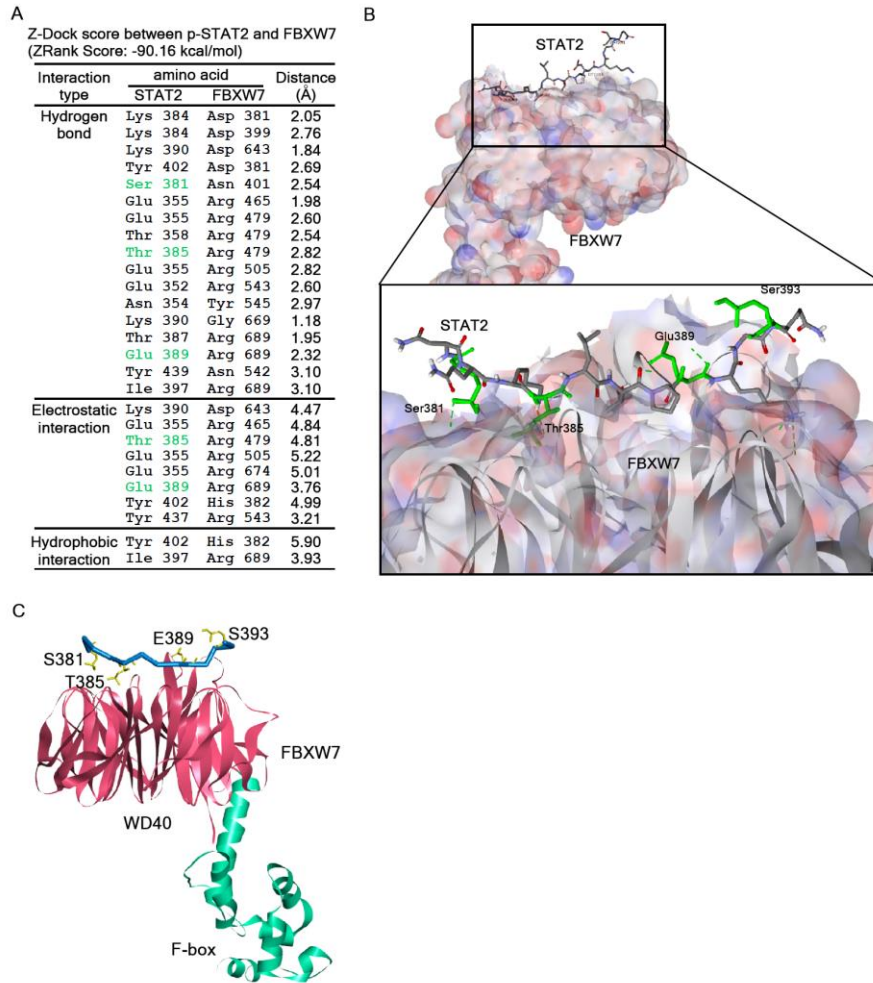
SI Appendix, Figure S2

Z-Dock score between STAT2 and FBXW7
(ZRank Score: -48.49 kcal/mol)

Interaction type	amino acid				Distance (Å)
	STAT2		FBXW7		
Hydrogen bond	Arg	343	Asp	689	2.81
	Asn	354	Tyr	545	3.38
	Ser	381	Asp	399	2.64
	Tyr	439	Asn	542	2.33
	Glu	355	Arg	465	3.17
	Gln	352	Arg	543	2.97
	Thr	438	Arg	543	2.96
	Lys	390	Gly	669	2.81
	Glu	389	Arg	689	2.43
	Gly	395	Arg	689	2.58
	Glu	389	Asn	690	2.50
Ser	381	Asp	400	3.10	
Electrostatic interaction	Lys	390	Asp	643	4.57
	Glu	352	Arg	543	5.56
	Glu	389	Arg	689	3.37
	Tyr	437	Arg	543	2.33
	Lys	390	Asp	643	4.57
Hydrophobic interaction	Trp	384	His	382	5.03

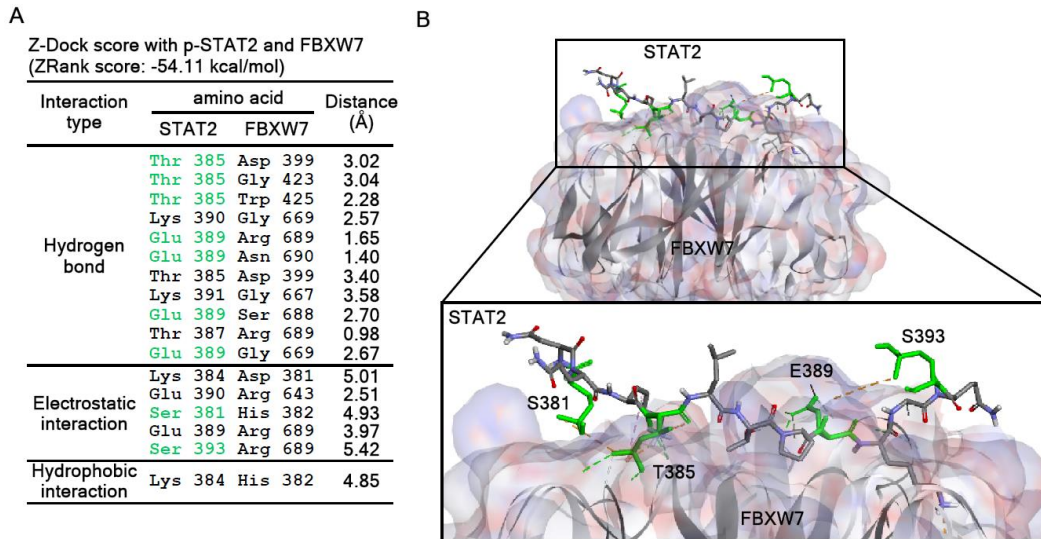
SI Appendix, Figure S2. A STAT2 and FBXW7 docking model showing that non-phospho-amino acids in degreon motifs interacted with WD40 domain of FBXW7. The list of interaction types between non-phospho-amino acids in STAT2 degreon motifs and WD40 domains of FBXW7. The Z rank score means the binding energy in kcal/mol. The atomic distance for bond formation is denoted as Å.

SI Appendix, Figure S3



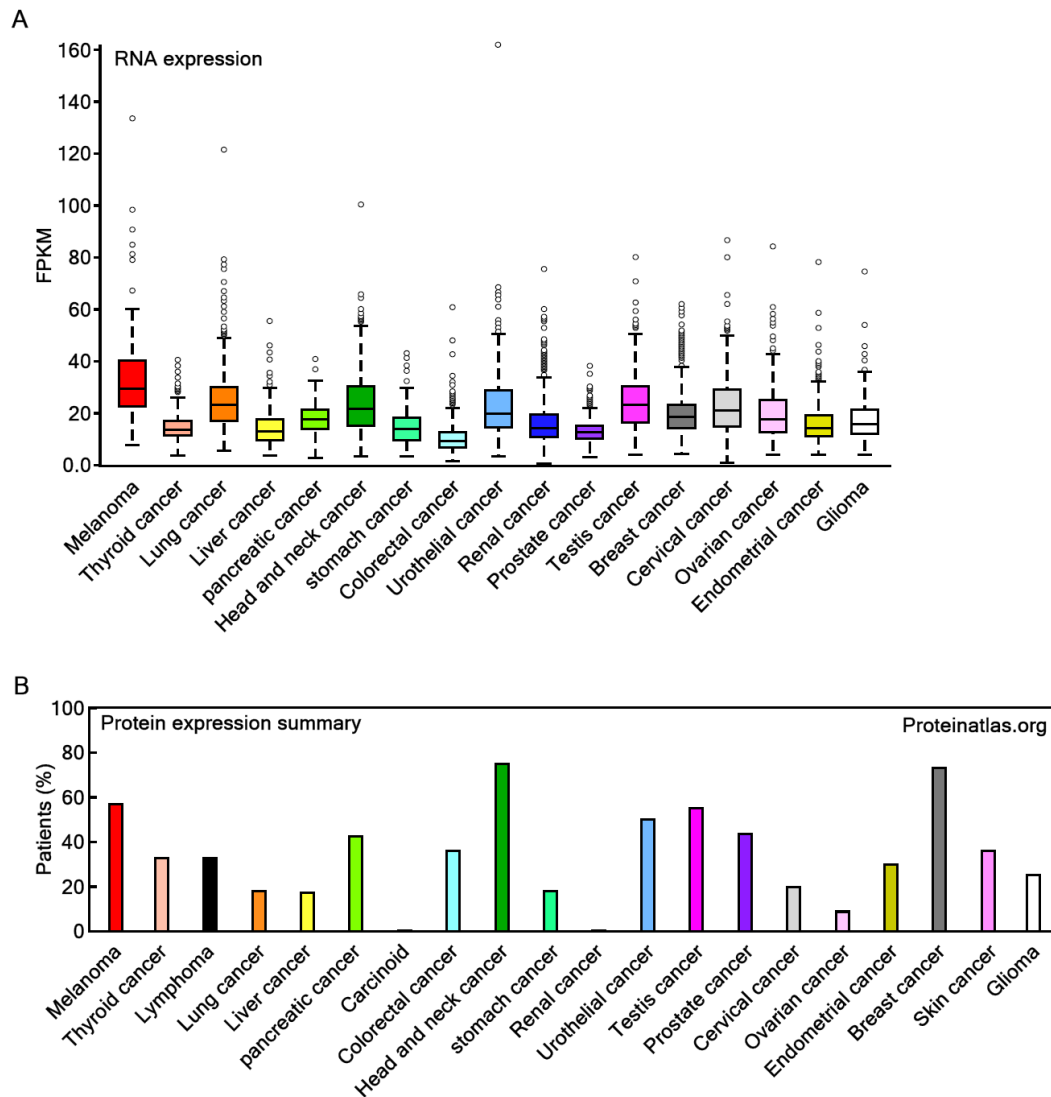
SI Appendix, Figure S3. A STAT2 and FBXW7 docking model showing that exchange of phospho-amino acids in degnon motifs reduced binding energy provided by interaction between STAT2 and FBXW7. (A) The list of interaction types between phospho-amino acids in STAT2 degnon motifs and WD40 domain of FBXW7. The Z rank score means the binding energy in kcal/mol. Atomic distances for bond formation is denoted as Å. (B) Closed view of the interaction surface between the phospho-amino acids of the degnon motifs in STAT2 and WD40 domains of FBXW7. Here, the stick indicates the amino acid backbone, green indicates amino acid side chains of STAT2 formed hydrogen bonds FBXW7, and blue indicates the side chains of each amino acid in the degnon motifs of STAT2. FBXW7 denotes the protein surface. The dotted lines indicate the hydrogen bonds between phospho-amino acids of degnon motifs in STAT2 and WD40 domains of FBXW7. (C) Structural view for phospho-amino acids of the degnon motifs in STAT2 to determine the orientation of the side chain in phospho-Ser393 for the degnon motifs of STAT2.

SI Appendix, Figure S4



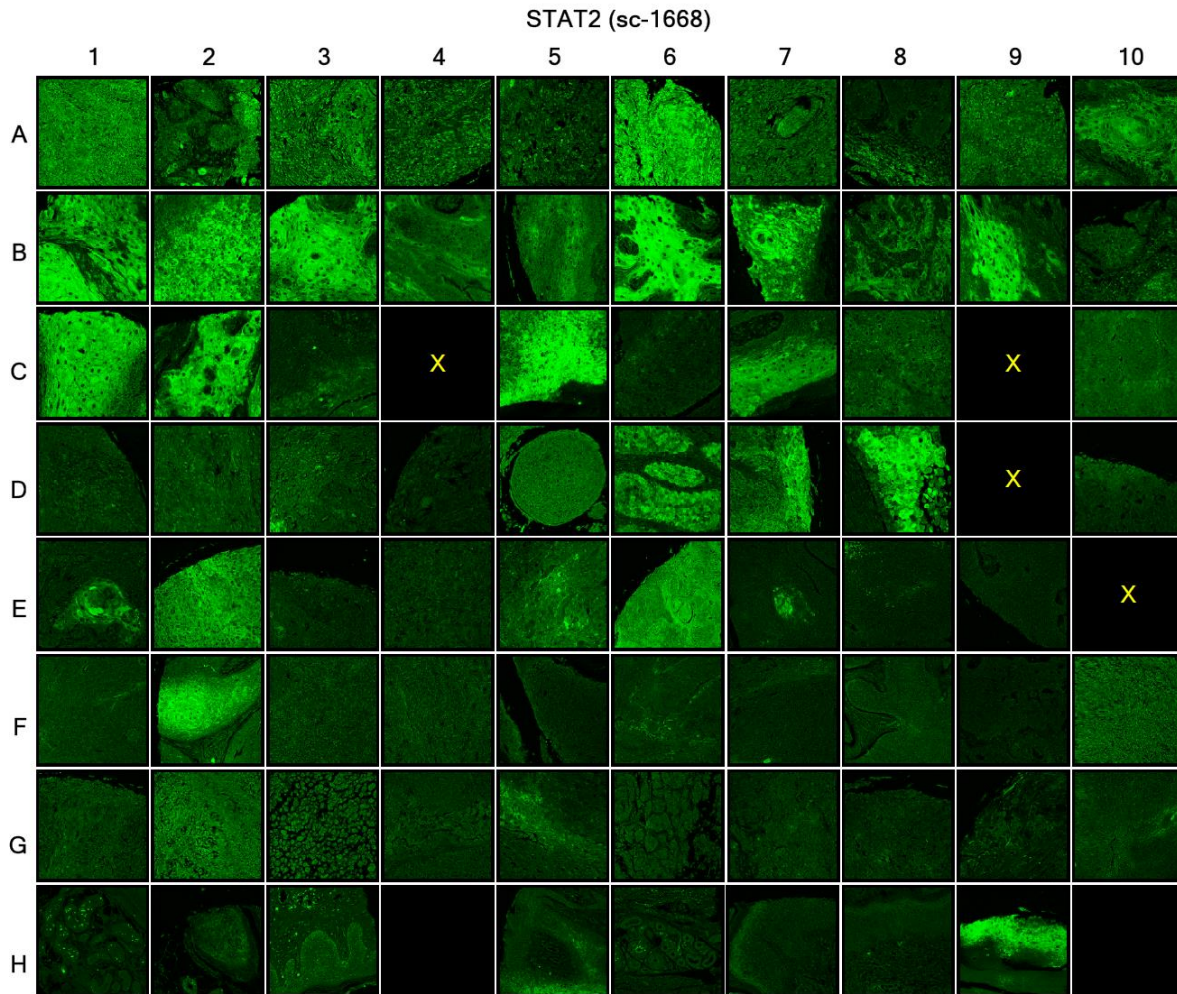
SI Appendix, Figure S4. Refinement of a STAT2 and FBXW7 docking model showing that phospho-Ser381, -Thr385, -Ser393, and Glu389A in STAT2 can participate in the interaction between STAT2 and FBXW7. (A) The list of interaction types between phospho-amino acids in STAT2 degnon motifs and WD40 domain of FBXW7. The Z rank score means the binding energy in kcal/mol. Atomic distance for bond formation is denoted as Å. (B) Refined closed view of interaction surface between the phospho-amino acids of degnon motifs in STAT2 and WD40 domains of FBXW7. The stick indicates the amino acid backbone, and the blue stick indicates the side chains of each amino acid in the degnon motifs of STAT2. FBXW7 denotes the protein surface. The dotted lines indicate the hydrogen bonds between phospho-amino acids of the degnon motifs in STAT2 and the WD40 domains of FBXW7. Refined structural view for phospho-amino acids of the degnon motifs in STAT2 shows the orientation of the side chain of phospho-Ser393 in the degnon motifs of STAT2.

SI Appendix, Figure S5



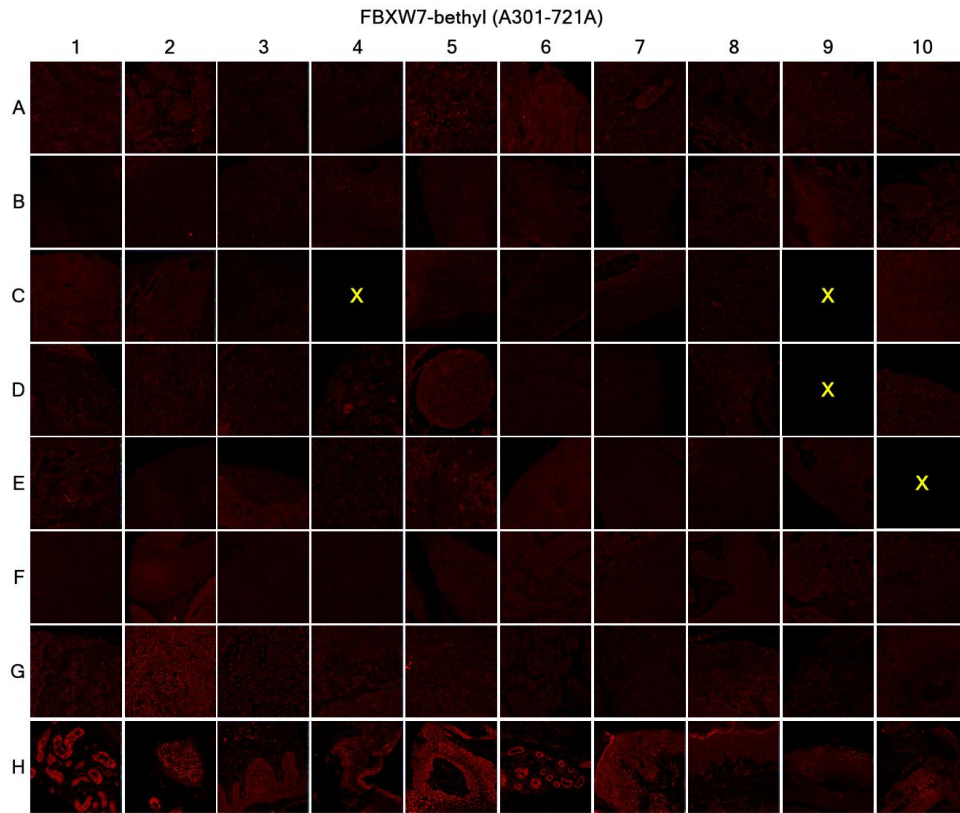
SI Appendix, Figure S5. The mRNA and protein levels of STAT2 in melanoma tissues. (A) The mRNA expression of STAT2 was obtained via RNA-seq data generated by the Cancer Genome Atlas (TCGA) using 17 cancer types. (B) The protein content of STAT2 in different cancer types in human. The data was obtained from the Human Protein Atlas database (www.proteinatlas.org).

SI Appendix, Figure S6



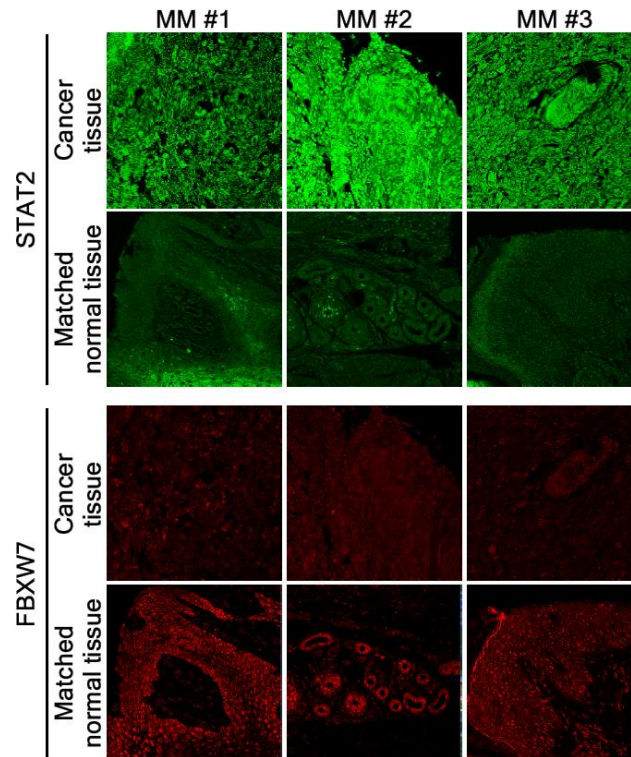
SI Appendix, Figure S6. Human skin tissues contain relatively higher levels of STAT2 protein than normal tissues. Human skin tissue arrays were conducted using human skin tissue array set (SK801), which contained 70 human skin cancer tissues and 10 normal tissues. The fluorescence intensity was measured using Image J (NIH Image J ver. 1.52). The STAT2 protein levels in each tissue sample is provided in Figure 7A in the main text. Detailed information including age, sex, grade, and other characteristics can be found at Biomax us (<https://www.biomax.us/tissue-arrays/Skin/SK801>).

SI Appendix, Figure S7



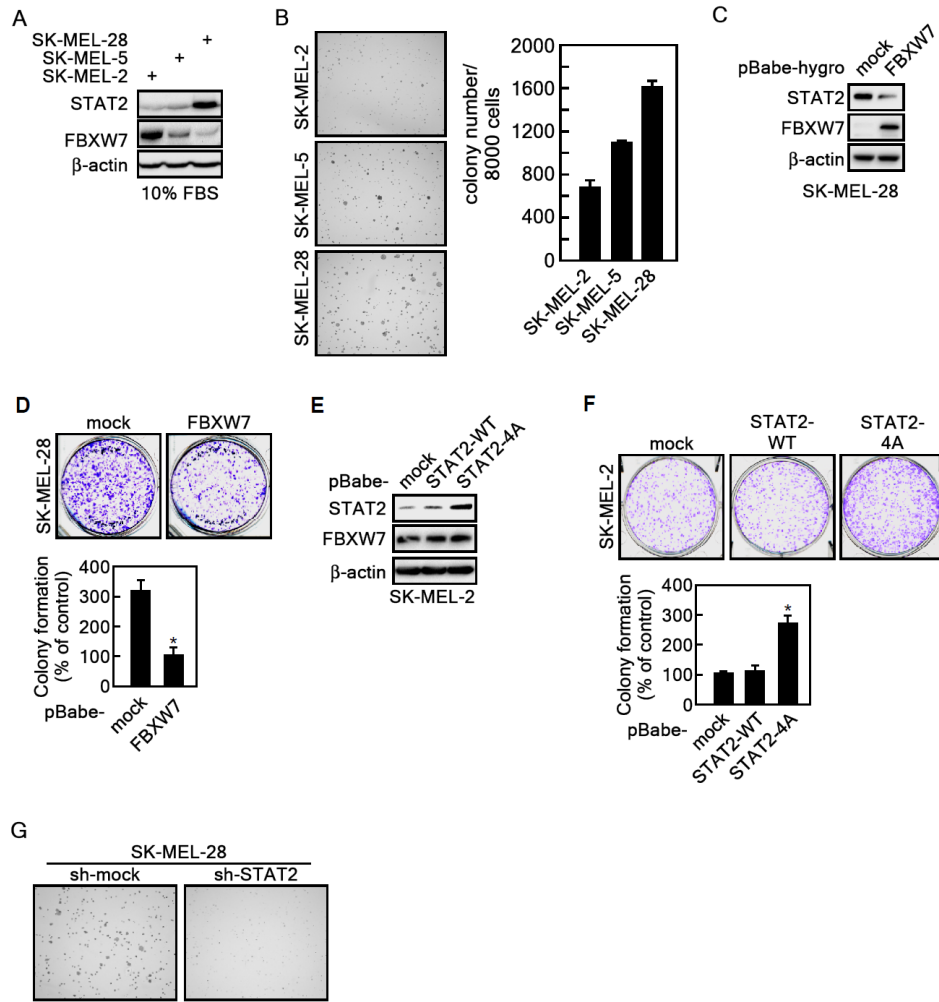
SI Appendix, Figure S7. Human skin tissues contain relatively higher levels of FBXW7 protein than normal tissues. Human skin tissue arrays were conducted using human skin tissue array set (SK801), which contained 70 human skin cancer tissues and 10 normal tissues. The fluorescence intensity was measured using Image J (NIH Image J ver. 1.52). The FBXW7 protein levels in each tissue sample is provided in Figure 7A in the main text. Detailed information including age, sex, grade, and other characteristics can be found at Biomax us (<https://www.biomax.us/tissue-arrays/Skin/SK801>).

SI Appendix, Figure S8



SI Appendix, Figure S8. Analysis of STAT2 and FBXW7 protein levels in matched human skin cancer and normal tissues. The SK801 human skin tissue array set contained matched human skin tissues that were biopsied from the same patient. The fluorescence intensity was measured using Image J (NIH Image J ver. 1.52). The fluorescence intensity was compared, and the relative intensity is presented in Figure 7C in the main text. Detailed information for each tissue sample including age, sex, grade, and other characteristics can be found at Biomax us (<https://www.biomax.us/tissue-arrays/Skin/SK801>).

SI Appendix, Figure S9



SI Appendix, Figure S9. STAT2 induces colony growth of melanoma cells. (A) WB analysis of WCLs derived from human melanoma cell lines SK-MEL-28, SK-MEL-5, and SK-MEL-2. (B) Anchorage-independent colony growth of melanoma cells. *Left panels*: Representative photographs for anchorage-independent colony growth of melanoma cells. *Graph*; average colony numbers obtained from triplicate 6-well plates. (C) Representative photographs to determine the ectopic expression of FBXW7 in SK-MEL-28 melanoma cells. (D) Foci formation assay to determine the effect of FBXW7 overexpression in SK-MEL-28 melanoma cells. *Upper panels*; representative photographs for colony growth by crystal violet staining. *Graph*; average colony numbers obtained from triplicate 6-well plates. (E) Representative photographs to determine the ectopic expression of STAT2-WT or STAT2-4A mutant protein in SK-MEL-2 melanoma cells. (F) Foci formation assay to determine the effect of STAT2-WT or STAT2-4A mutant overexpression in SK-MEL-2 melanoma cells. *Upper panels*; representative photographs for colony growth

by crystal violet staining. *Graph*; average colony numbers obtained from triplicate 6-well plates. (*G*) Representative photographs for the effects of STAT2 knockdown on the anchorage-independent colony growth in SK-MEL-28 cells. (*C*, *E*, *G*, and *H*) Colony numbers were counted using an ECLIPSE Ti inverted microscope and analyzed by NIS-Elements AR (V. 4.0) software.

5. Si Appendix, Whole blots

Fig.1

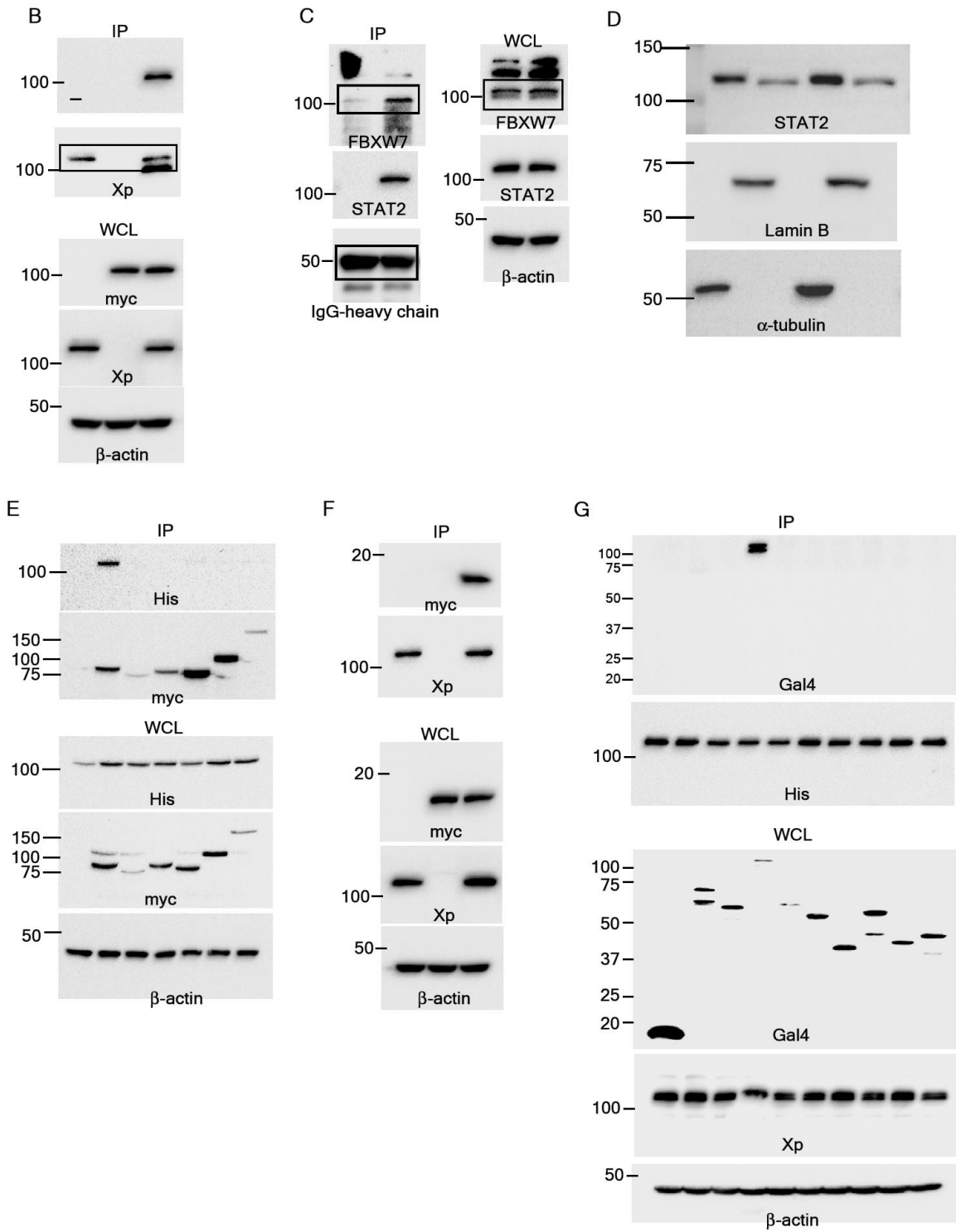


Fig.2

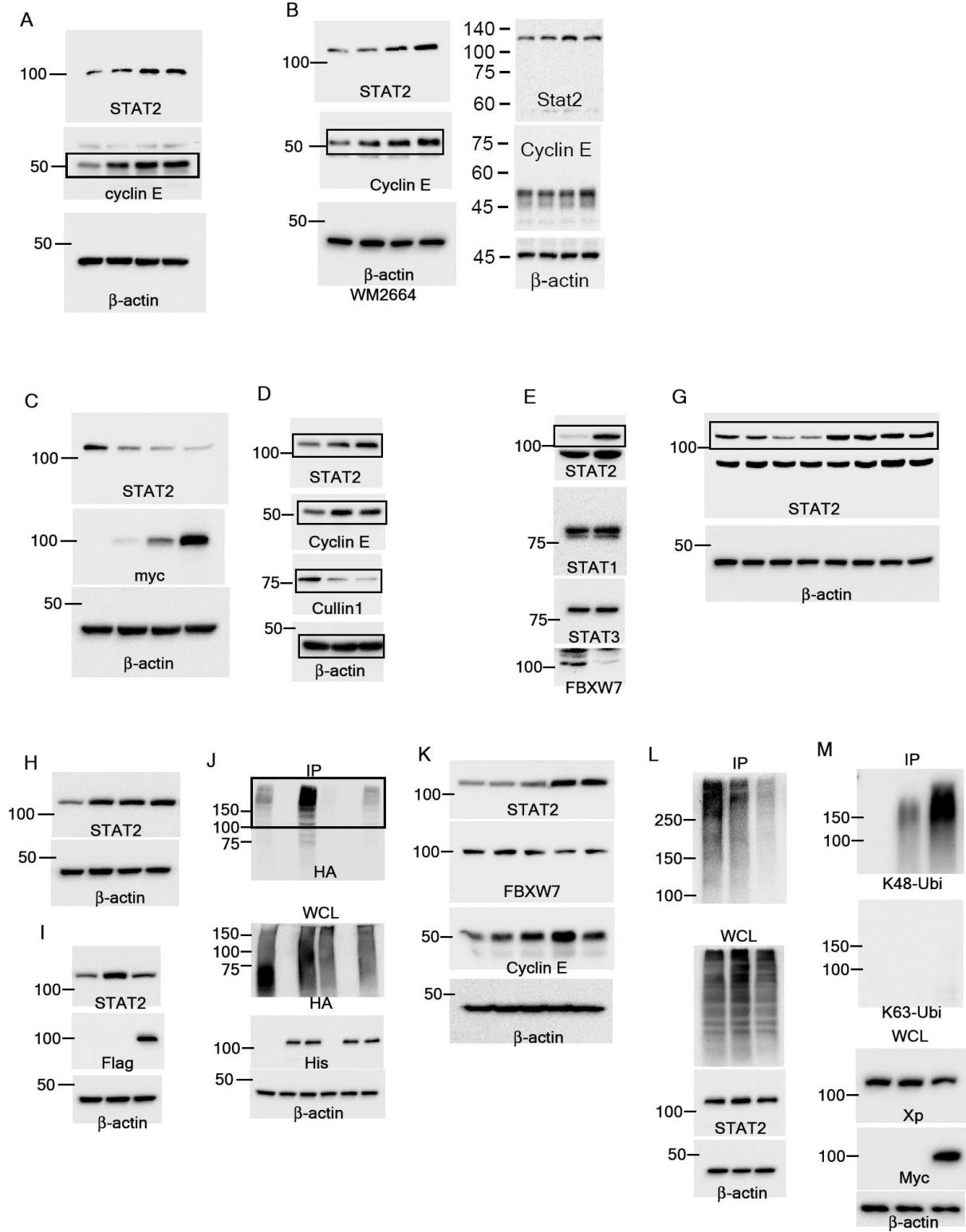


Fig.3

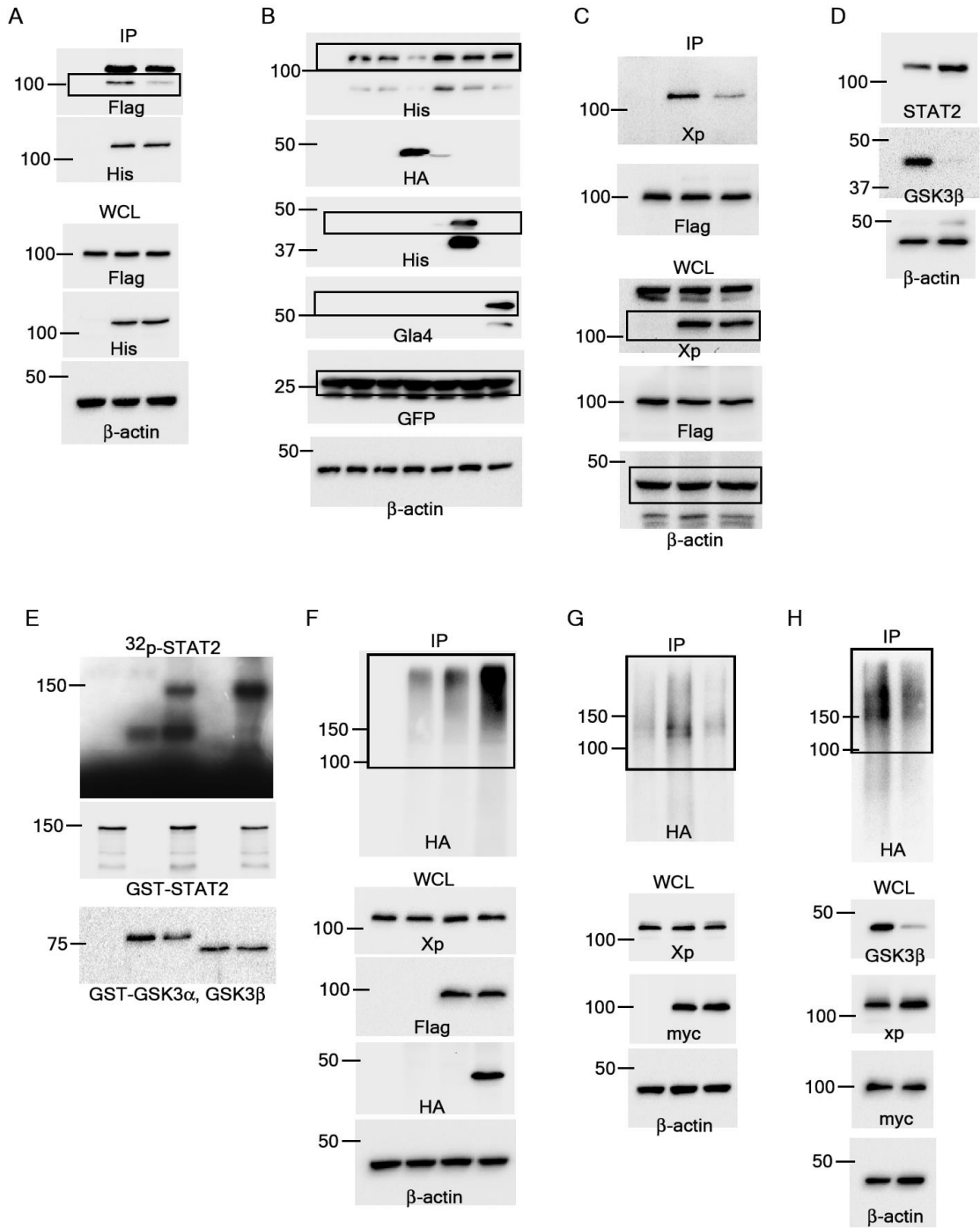


Fig.4

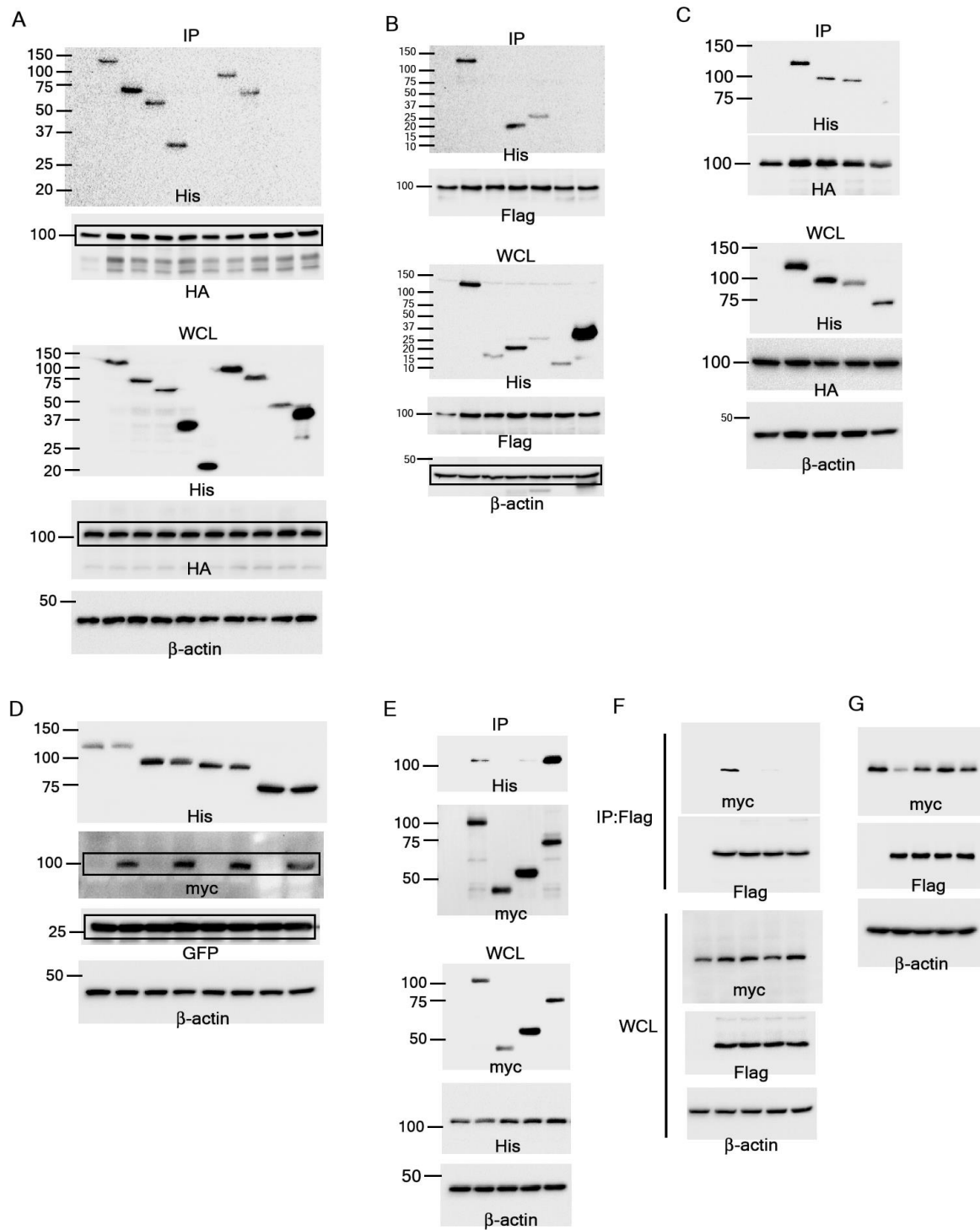


Fig.5

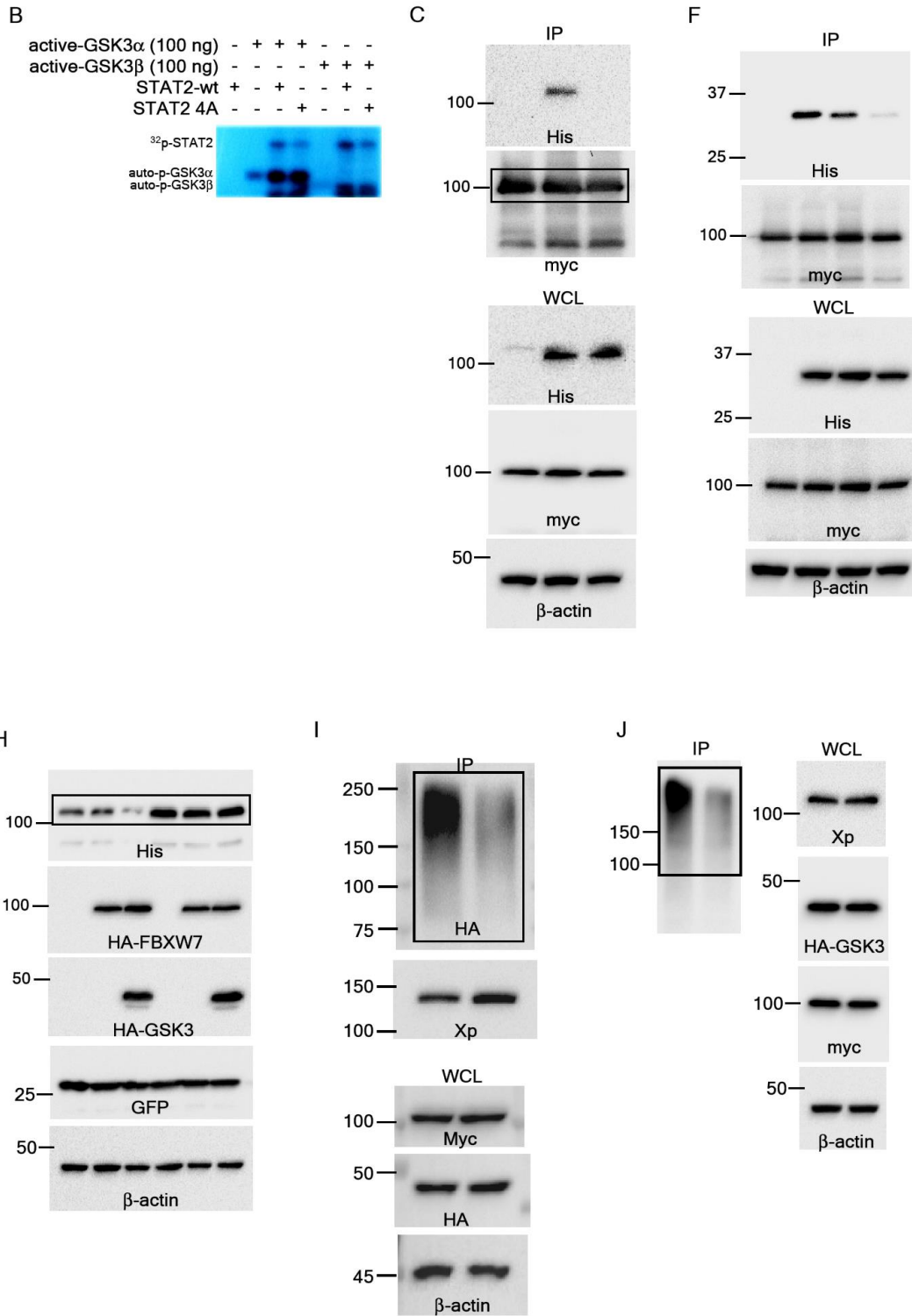
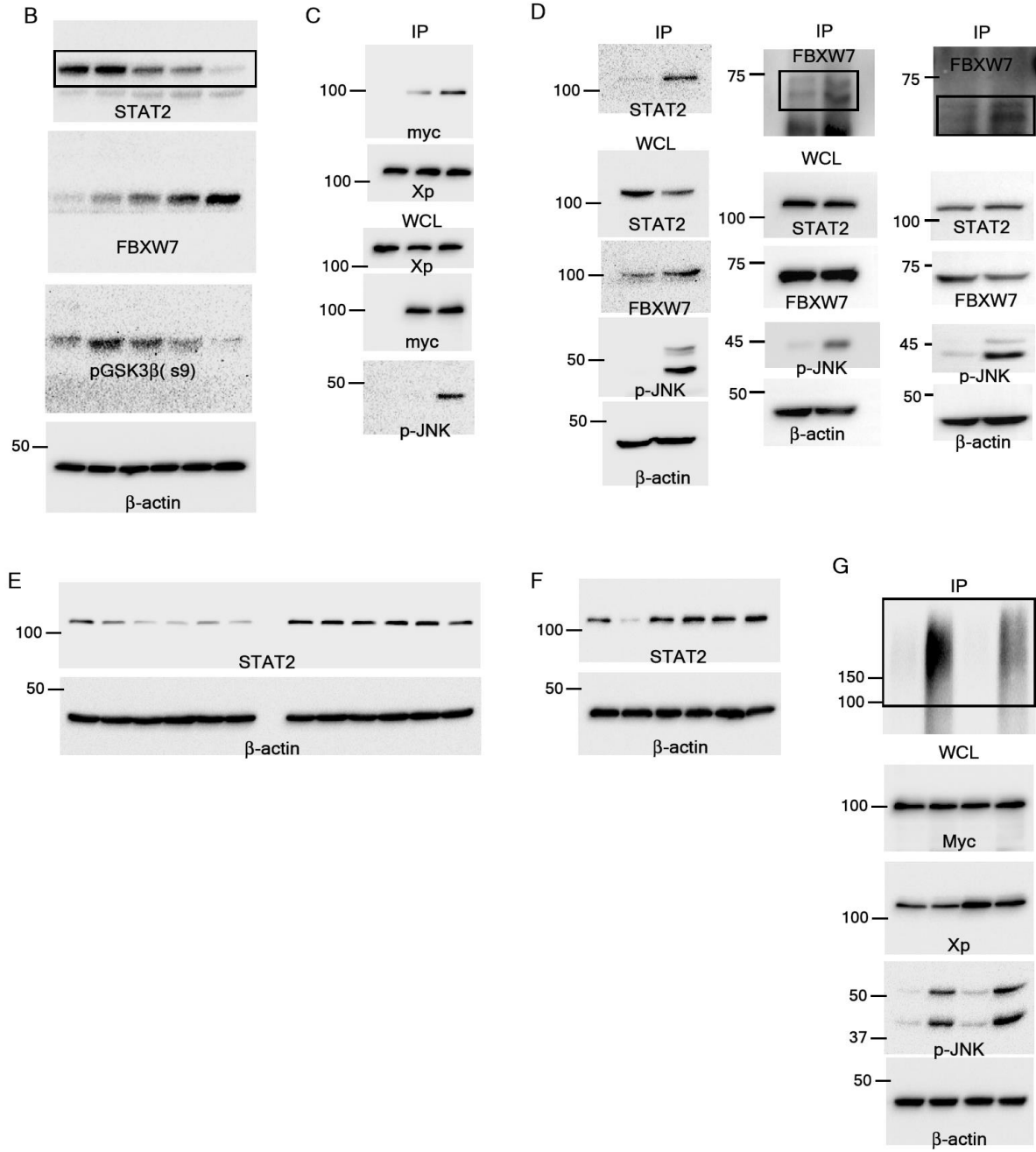


Fig.6



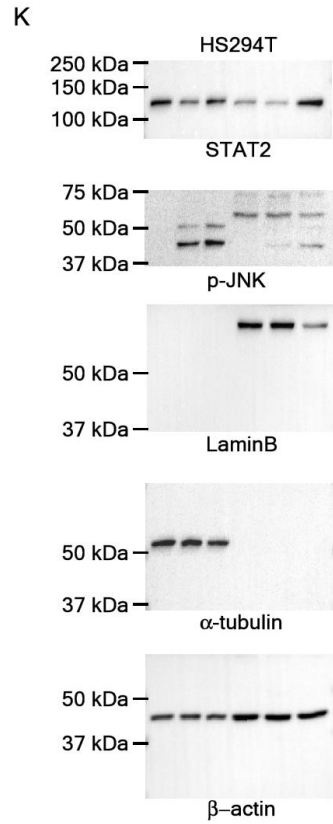
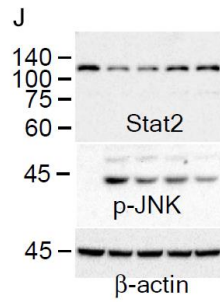
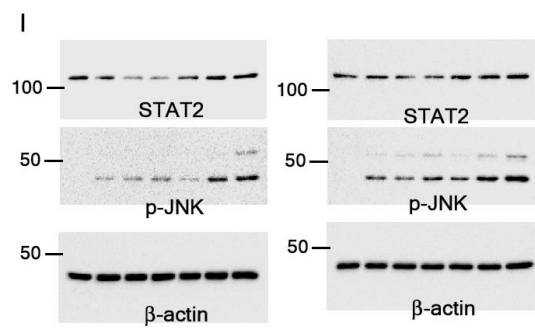
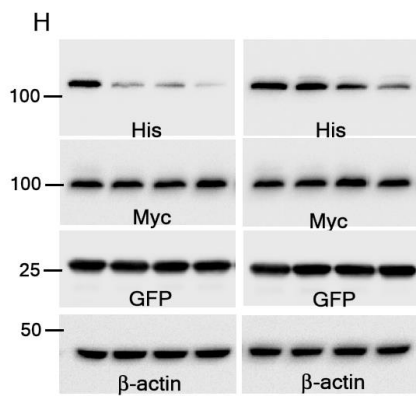
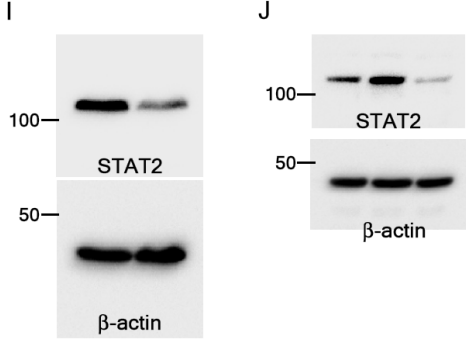


Fig.7



SI Dataset S9

